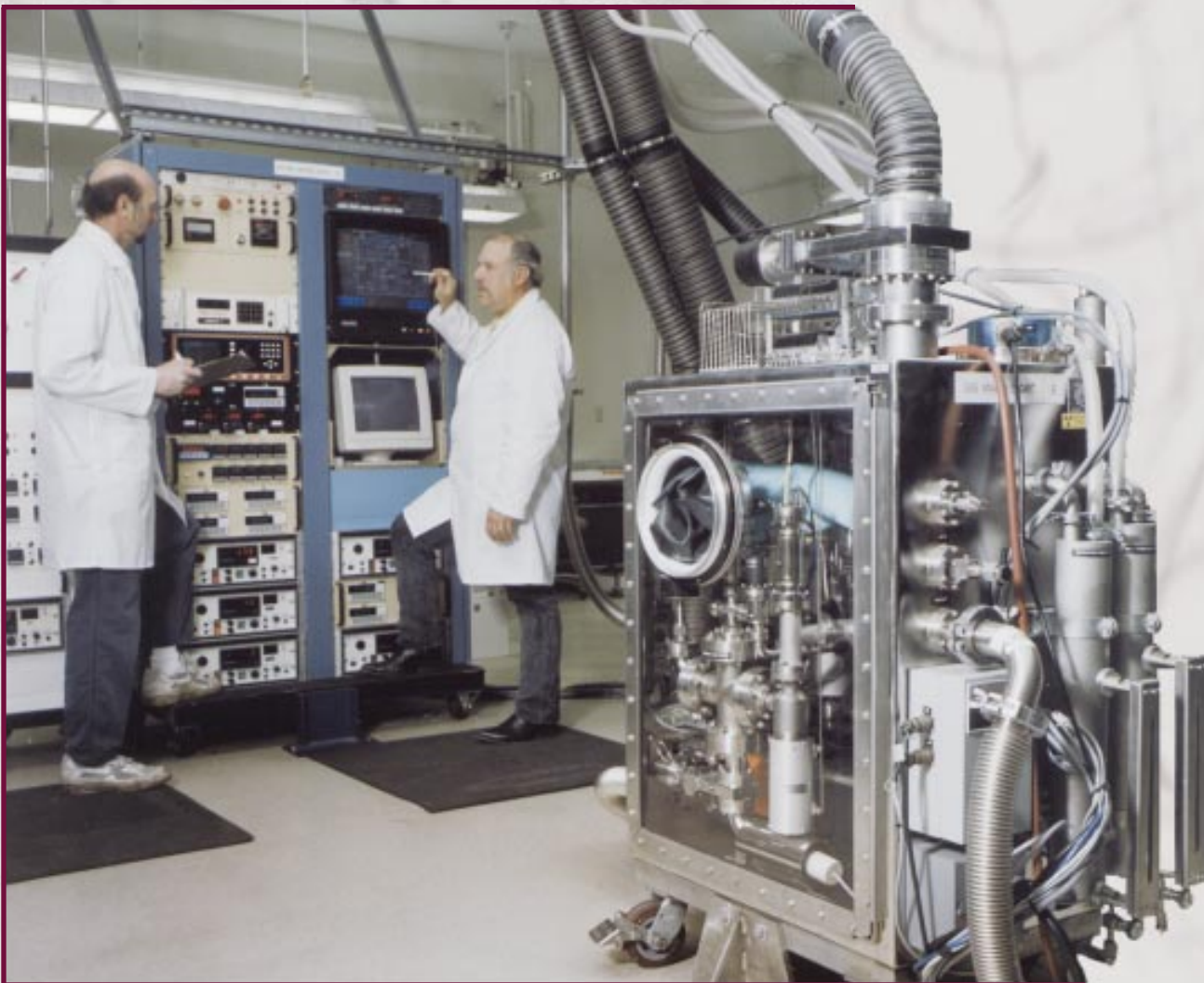
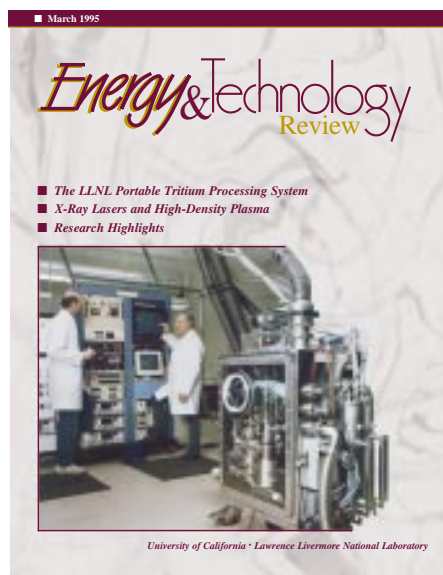


Energy & Technology Review

- *The LLNL Portable Tritium Processing System*
- *X-Ray Lasers and High-Density Plasma*
- *Research Highlights*





About the Cover

This month's cover story (see p. 1) reports on the background, design, and capabilities of the Portable Tritium Processing System (PTPS) currently being used to clean up and decontaminate the Laboratory's Tritium Facility under the Tritium Inventory Removal Project. The PTPS has four parts: a gas pumping and transport module, a gas analysis module, a scrubbing module, and a computerized operation and control module. Each is portable in the sense that it can be moved from place to place in the Tritium Facility and reconnected to the other modules for tritium gas recovery, analysis, decontamination, and cleanup. Mike Benapfl (left) and Vern Switzer are pictured working at the computerized operation and control module, which permits semi-automatic remote activation of the other three system modules. In the foreground is the gas analysis module where the gas species (tritium as well as other gases) are identified at subatmospheric pressure and routed by the computer module operators to the correct location within the processing system for appropriate treatment and containment. The PTPS has been designed and built to the most stringent standards of worker and environmental protection.



Prepared for **DOE** under contract
No. W-7405-Eng-48

About the Journal

The Lawrence Livermore National Laboratory, operated by the University of California for the United States Department of Energy, was established in 1952 to do research on nuclear weapons and magnetic fusion energy. Since then, in response to new national needs, we have added other major programs, including laser science (fusion, isotope separation, materials processing), biology and biotechnology, environmental research and remediation, arms control and nonproliferation, advanced defense technology, applied energy technology, and industrial partnerships. These programs, in turn, require research in basic scientific disciplines, including chemistry and materials science, computing science and technology, engineering, and physics. The Laboratory also carries out a variety of projects for other federal agencies. *Energy and Technology Review* is published monthly to report on unclassified work in all our programs. Please address any correspondence concerning *Energy and Technology Review* (including name and address changes) to Mail Stop L-3, Lawrence Livermore National Laboratory, P.O. Box 808, Livermore, CA 94551, or telephone (510) 422-4859, or send electronic mail to etr-mail@llnl.gov.

■ March 1995

SCIENTIFIC EDITOR
William A. Bookless

PUBLICATION EDITOR
Dean Wheatcraft

WRITERS
Kevin Gleason, Robert D. Kirvel

DESIGNER
Kathryn Tinsley

ILLUSTRATOR
Trevia Carey

COMPOSITOR
Louisa Cardoza

PROOFREADER
Catherine M. Williams

This document was prepared as an account of work sponsored by an agency of the United States Government. Neither the United States Government nor the University of California nor any of their employees makes any warranty, expressed or implied, or assumes any legal liability or responsibility for the accuracy, completeness, or usefulness of any information, apparatus, product, or process disclosed, or represents that its use would not infringe privately owned rights. Reference herein to any specific commercial product, process, or service by trade name, trademark, manufacturer, or otherwise does not necessarily constitute or imply its endorsement, recommendation, or favoring by the United States Government or the University of California. The views and opinions of authors expressed herein do not necessarily state or reflect those of the United States Government or the University of California and shall not be used for advertising or product endorsement purposes.

Printed in the United States of America
Available from
National Technical Information Service
U.S. Department of Commerce
5285 Port Royal Road
Springfield, Virginia 22161

UCRL-52000-95-3
Distribution Category UC-700
March 1995

Energy & Technology Review

Feature Articles

The LLNL Portable Tritium Processing System

1

We have miniaturized current tritium processing technology for removing tritium from facilities and decontaminating them and have packaged the technology in modular units that are self-contained, easily transportable, and usable in confined spaces.

X-Ray Lasers and High-Density Plasma

9

We are developing the laboratory x-ray laser as a probe to obtain high-resolution images of high-density plasmas produced at the Nova laser facility. Three techniques and future applications are described.

Research Highlights

Silicon Carbide Microcomponents

20

Modern Technology for Advanced Military Training

22

Abstracts

25

The LLNL Portable Tritium Processing System



The system is made up of modular units that provide tritium pumping, analysis, and effluent scrubbing capabilities. The units are sized to pass through a standard-width doorway and have two containment layers for maximum safety.

THE end of the Cold War significantly reduced the need for facilities to handle radioactive materials for the U.S. nuclear weapons program. Many of these facilities were thus slated for decontamination and decommissioning. LLNL was among the institutions affected by these changed circumstances. Weapons program needs and funding were diminishing while costs for modernization as well as for routine operation were rapidly escalating.

In 1991, the Laboratory decided to close its Tritium Facility, a decision requiring inventory removal and decontamination. In the course of decades of Nuclear Weapons Program work, research was conducted on tritium and tritiated materials. Components using tritium were also developed for nuclear testing at the Nevada Test Site. Fusion energy

research, for which tritium is a key fuel, was also a major focus. Over the years, therefore, tritium and contaminated tritium processing systems had accumulated.

While the decision to close the facility was later reconsidered, the facility's new and ongoing activities in tritium and decontamination research and development continued to require decontamination of its laboratories and removal of most remaining tritium inventory. This process required removing the inventory of tritium within the facility and cleaning up any pockets of high-level residual contamination.

The tritium handling systems at the facility needed to be updated and improved to perform the task of decontamination and decommissioning within today's stringent standards of worker and environmental protection.

For example, most such systems had only a single barrier between the system's interior and the laboratory work environment. Today's standards also require more stringent controls of tritium release than in the past.

A project group was formed to develop the best approach for removing the tritium inventory and decontaminating the facility. After considering a variety of inventory removal scenarios, the group decided to design and build a new tritium processing system to current, stringent guidelines.

System Capabilities

During the conceptual design phase, the team identified four basic functions that the system must perform to achieve complete inventory removal. It must:

- Evacuate the facility’s gas-handling systems, vessels, and plumbing in preparation for disassembly.
- Analyze the composition of the extracted gases.
- Scrub, or remove, tritium from residual gases.
- Transfer tritium from one container to another or to a shipping vessel that can be sent to another Department of Energy facility for tritium recovery.

In order to be used in the confined spaces of the building that housed LLNL’s Tritium Facility, the system would have to be portable so that it could be moved from laboratory to laboratory and could fit into, and work effectively in, confined spaces. The system could therefore be no wider than a standard 36-inch-wide laboratory door.

Designing the System

The combined performance and size criteria for the system posed a major design challenge, because a

system using current technology and meeting current standards would ordinarily fill a sizable room. After consultations and reviews with tritium experts at LLNL, Sandia National Laboratory, and EG&G Mound Applied Technologies, LLNL established the basic design for the Portable Tritium Processing System (PTPS). The design uses current, well-proven tritium-processing technology, but with process components miniaturized and packaged to meet the portability and access requirements. For this reason, the system was divided into three separate modules that, when installed together, provide the required processing capabilities: pumping/transfer, analysis of the gas constituents, and removal of tritium. **Figure 1** shows a schematic drawing of such a system’s functions and components.

An additional design challenge was posed by the requirement that the system modules operate in a variety of circumstances within today’s

stringent release criteria. The solution was to design the system with two layers of containment. The system’s process plumbing (e.g., pumps, tanks, pressure transducers, valves, flow meters, catalytic reactors, and heat exchangers) would be sealed against leaks (see **Figure 2a**). The plumbing would be further isolated by a secondary containment layer designed to employ the latest technology for building a glovebox (a sealed box with gloves protruding into it for workers to use in handling materials, such as radioactive substances). Built of 3/16-in. stainless steel with Lexan windows and commercially manufactured gloveports (see **Figure 2b**), the secondary enclosure of each module is also equipped with a tritium detector to monitor for potential leaks in the process plumbing.

Gloveboxes provide their protection not only by virtue of the sealed mechanical barrier of steel, Lexan, and gloveports, but also by

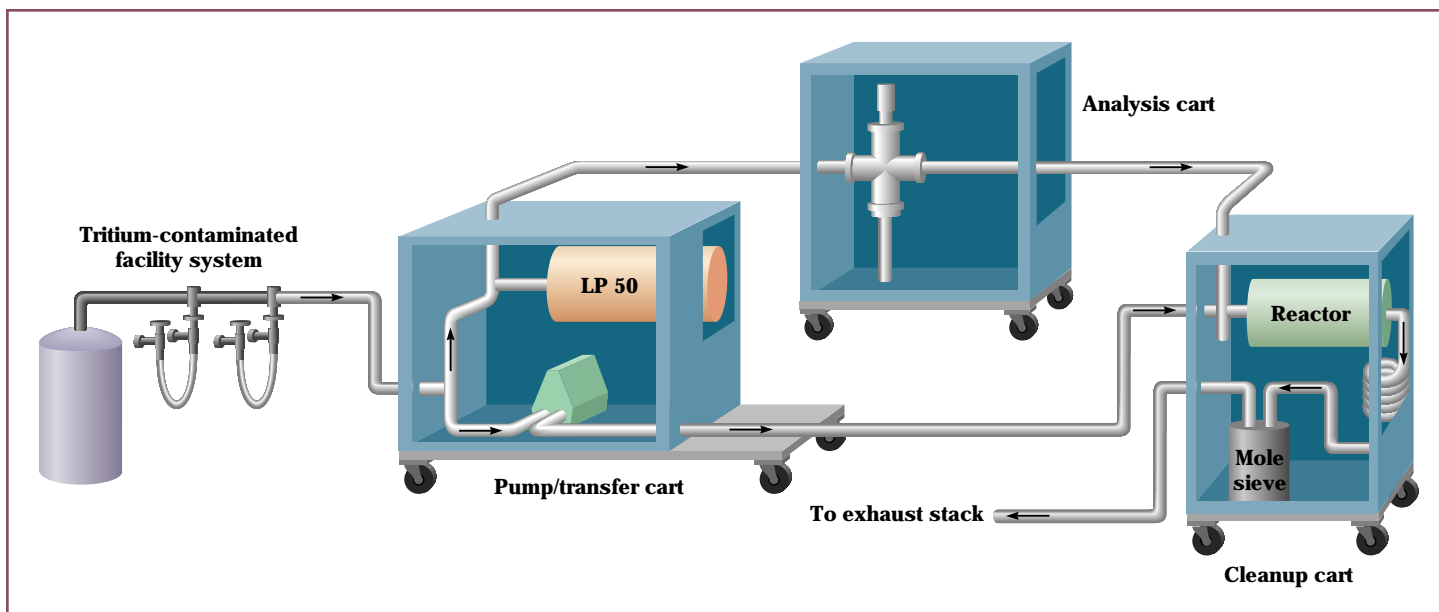


Figure 1. Schematic of the Portable Tritium Processing System (PTPS) showing the three modules and their connecting plumbing.

allowing the atmosphere within the box to be maintained at less than atmospheric pressure. If the box develops a leak, room air will enter the box rather than contaminants leaking out. Indeed, the process plumbing typically operates at vacuum—0.5 Torr (atmospheric pressure at sea level is equivalent to 760 Torr).

Enclosing all process plumbing and hardware in modules presented additional design problems. Several components, such as the catalytic reactor in the scrubber module, generate heat that must be dissipated so that an overpressure (pressure exceeding the set point) does not build up within the enclosures. Such an overpressure could cause a release to the environment and/or damage system instruments. We designed two of the three modules—the analysis and scrubber modules—with ventilation ports that remain open under normal operating conditions. In the event that a tritium detector senses a leak from the process plumbing in these two modules, the ventilation ports close automatically. To prevent an overpressure buildup in the scrubber module when it operates without ventilation, the heat-generating components are insulated so that they release heat at a lower rate than it can be dissipated.

The secondary enclosure of the pump/transfer module is not ventilated during operation. With a maximum allowable working pressure of only 0.22 psi (pounds per square inch), a leak in the process plumbing during operation could easily create an overpressure. To resolve this potential problem, we added two additional levels of protection against overpressurization of the secondary enclosure. The first is a diverter, or abort, system that uses a series of pressure detectors and valves and an

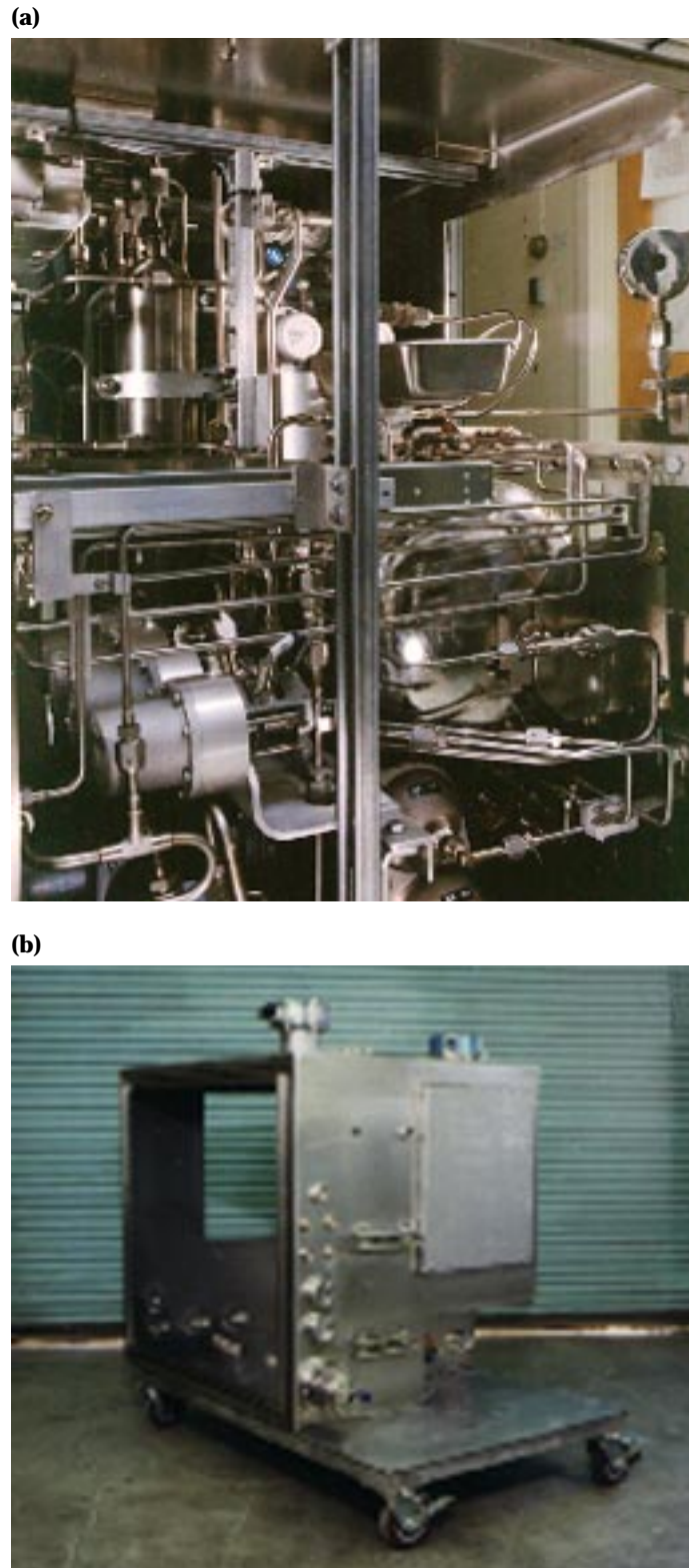


Figure 2. (a) Part of the primary enclosure system in the pump/transfer module. (b) The steel shell of the pump/transfer secondary enclosure while under construction. Any leak resulting from failure or compromise of the primary system will be contained by this enclosure.

evacuated tank. If excess pressure is detected, the valves divert excess gas to the tank. Although the set point is 0.22 psi, the detectors activate the diverter system at 0.036 psi to give the system time to react. If analysis of the diverted gas determines that tritium is present, the gas can be held in the abort tank for later processing. The second pressure-relief system consists of commercial oil-sealed bubblers. In the extremely unlikely event that the primary abort system fails, the bubblers vent the excess gas to the exhaust stack, protecting the operators from any harmful constituents in the gas.

To prevent oil contamination of recoverable tritium and internal process plumbing, the pump/transfer and scrubber modules use oil-free pumps. The pump/transfer module uses a metal

bellows-type pump in combination with a scroll pump, producing the base pressure of 0.5 Torr. To minimize the possibility of combustion within the pump/transfer module, all electrical spark sources have been located outside the enclosure, including the motors driving the pumps.

The processing system is operated by dual control. A few valves are operated manually, but the rest of the system is operated from a central console, which allows for remote operation of the process modules as space constraints or circumstances require (see [Figure 3](#)). The console uses a programmable logic controller to initiate user commands as well as to monitor system status and to automatically activate process-control interlocks that prevent internal pressures, temperatures, and tritium

levels from exceeding the system's handling capacities. If the console fails, the manual secondary control system can bring the system to a safe shutdown condition.

System Operation

A typical decontamination operation requires the use of all three modules—pump/transfer, gas-analysis, and scrubber—in combination with the central control console. The pump-transfer module provides the interface between the system and the manifolds or vessels to be emptied and decontaminated. Because gas pressure within the system to be analyzed is often unknown at the outset, the module inlet manifold has a working pressure of 200 psi (with an internal abort volume to which higher pressure gases would be diverted). As the gas enters the module's process plumbing, a series of electrical pressure transducers measures its pressure at points within the plumbing and relays the readings to the console.

Once the pressure has been determined, a sample is sent at subatmospheric pressure to the gas-analysis module, which houses a commercial quadrupole partial-pressure analyzer and pumping station (see [Figure 4](#)). The analyzer identifies the gas species present. Using the information relayed from the analyzer to the console, the operator routes the gas to the correct location within the processing system. The decision is based not only on tritium content but on other variables as well, such as the presence of combustible gas mixtures or of materials that would degrade the performance of the scrubber module. If the analysis indicates recoverable quantities of tritium, the gas is routed to bypass the scrubber



Figure 3. The control console gathers data from the modules, including temperature, pressure, gas species, and readings from the tritium monitors; automatic interlocks and shutdown systems operate from the console.

module and is pumped directly into a shipping vessel (see [Figure 5](#)) housed within the pump/transfer module (the vessel is a design approved by the Department of Transportation). If the analysis indicates the presence of a combustible mixture, the gas is diluted to a noncombustible state by being mixed with argon gas from the pump/transfer module.

Depending on its tritium content, the diluted gas mixture is either pumped to the shipping vessel in the pump/transfer module for later tritium recovery or is sent to the scrubber module for removal of the tritium. The scrubber removes the tritium by a succession of steps. First, the gas phase undergoes catalytic oxidation, which separates the hydrogen species, including tritium, from the other gas constituents and results in tritiated water (HTO). The tritiated water is collected on molecular sieve dryer beds—containers of minerals with spongelike structures. (See [Figure 6](#).) Two molecular sieve dryer beds are configured in series, each with its own downstream moisture monitor. When the monitor for the first bed indicates that the bed has become saturated, the operator stops the process and removes the saturated bed for disposal as low-level waste (less than 1000 curies of tritium). The second bed catches any vapor that passed through the first bed if the process was not stopped in time. The removed bed is replaced by the second bed, which is replaced by a fresh one.

Once the tritium inventory has been removed, the manifold can be further decontaminated in preparation for its removal. ([Figure 7](#) shows a typical manifold.) This step typically involves filling the old manifolds with room air and then flushing the

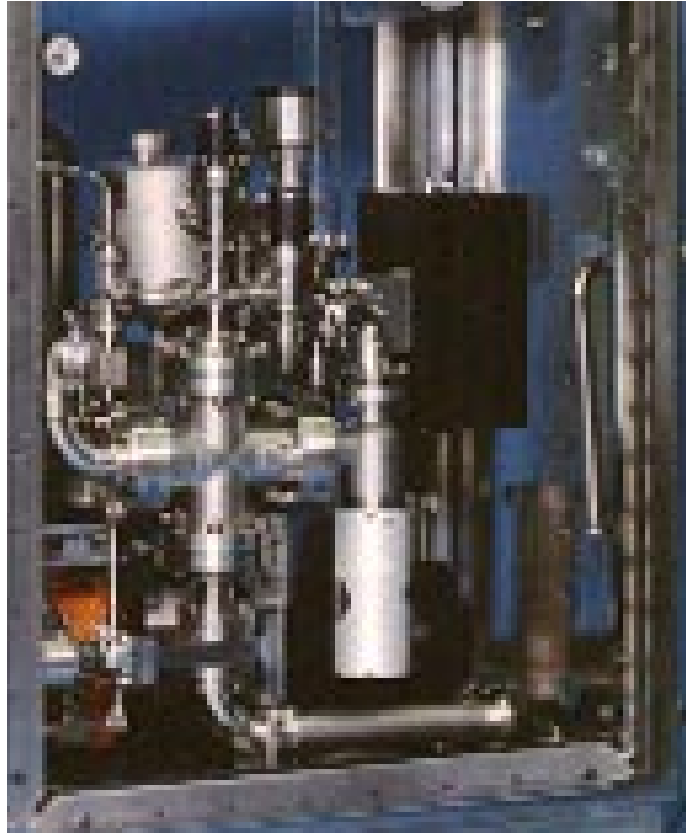


Figure 4. The gas analysis module. The quadrupole analyzer identifies not only tritium but species of combustible gas.

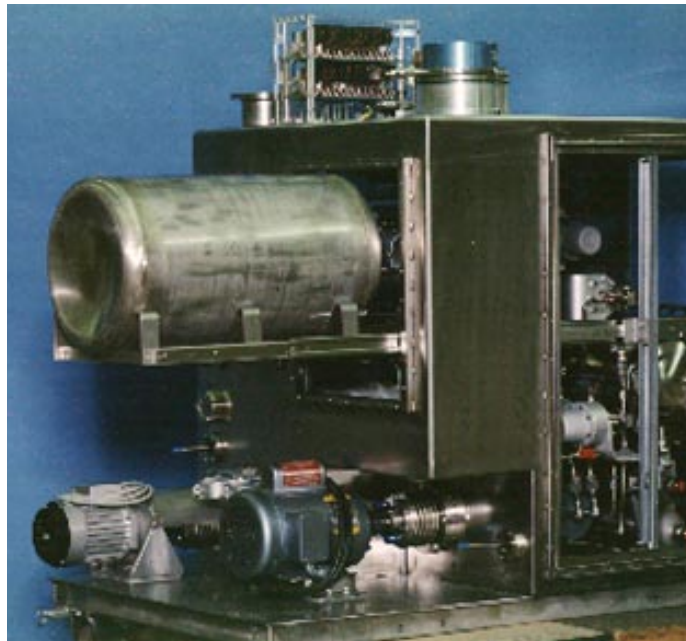


Figure 5. The pump/transfer module with a tritium shipping container resting on its cradle. Once the container has been inserted, the module enclosure is sealed.

air through the scrubber module until the tritium contamination is low enough to allow for safe disassembly. During the flushing, the inlet and outlet tritium monitors gauge the progress of decontamination.

The scrubber module can function on its own for cleaning large enclosures, such as gloveboxes. Additionally, in the event of a tritium leak into the secondary enclosure of the pump/transfer or gas-analysis module, the scrubber module evacuates and scrubs those gases. In the event that the scrubber module itself fails, a duplicate scrubber module can be used to clean up the failed scrubber. Once the failed scrubber is operating correctly again, normal processing can resume.

Figure 6. The scrubber module's catalytic reactor captures gaseous tritium as tritiated water, which is then collected on molecular sieve beds (lower left).



Tritium Inventory Removal Project

The Portable Tritium Processing System was specifically created to execute the Tritium Inventory Removal Project at the Laboratory. This project was designed to be performed in three phases. We have completed the first phase and are executing the second and third phases concurrently.

Phase 1 was the removal of tritium inventory. We consulted the Laboratory's materials management data base and defined anything containing 100 curies or more of tritium as an inventory item. We determined that there were approximately 14 grams of tritium inventory on hand, stored in several

forms—on metal (uranium or palladium) storage beds, bound up on titanium sponges and molecular sieves from old scrubber systems, in the gas phase in high-pressure vessels and old Department of Transportation shipping vessels, and in low-pressure vessels such as flush tanks, sample vials, etc. There were some 80 such inventory items, most connected to or contained within the old manifolds and systems.

Even after the inventory removal phase was completed, some 600 vessels and pieces of equipment remained to be investigated and processed, including approximately 250 detached vessels, 75 to 80 contaminated vacuum pumps of several types, and a few hundred canisters. A canister is a sealed atmospheric pressure vessel containing any of a variety of items—used molecular sieves, packages of waste, or titanium used in old purification systems.

These objects have been the focus of Phase 2. Because of their diverse characteristics and generally smaller size, most of them are better handled inside a glovebox. We have exploited the flexibility of our portable processing system by connecting it to a large, general-purpose glovebox, thereby giving it all the capabilities of our system: tritium monitoring, overpressure sensing, connection to the portable abort system, etc. (See [Figure 8](#).) The vessel being processed is connected to the pump/transfer module from inside the glovebox, so that were it to vent, the workers would be protected and the gas would be contained in the glovebox for processing by the scrubber module.

Once the processed vessels, pumps, and canisters are packaged for disposal as low-level waste and have been removed, the area is ready for Phase 3, which consists chiefly of disassembling and removing old manifolds and

gloveboxes. On completion of Phase 3, the Tritium Facility will have been decontaminated to a level consistent with its future mission.

Summary

LLNL has fabricated a portable tritium processing system that is completely self-contained. It is small enough to pass through a standard-width door so that it can be moved from laboratory to laboratory to perform basic tritium-processing operations. These operations include oil-free pumping and gas transfer, gas analysis, and gas-phase tritium



Figure 7. This complex gridlike structure of piping, valves, and gauges is one of the many manifolds in the LLNL Tritium Facility that have been decontaminated and disassembled.

(a)



(b)



Figure 8. (a) For Phase 2 of the Tritium Inventory Removal Project, the PTPS is connected to a general-purpose glovebox where smaller tritium-containing vessels and tritiated equipment can be examined and manipulated before analysis and treatment by the system's modules. (b) Vern Switzer works in the glovebox to clean out the final tubes of a disassembled facility prior to gas analysis, transfer, and processing.

scrubbing. The system is made up of three separate modules that are built to present glovebox standards and that perform complementary tasks: pumping gases from storage systems, analyzing them, and directing them for shipping or scrubbing, according to their tritium content. The system is operated from a portable console.

While the portable system continues to be the workhorse of the Tritium Inventory Removal Project, now in its final year, strong demand for tritium services has led to

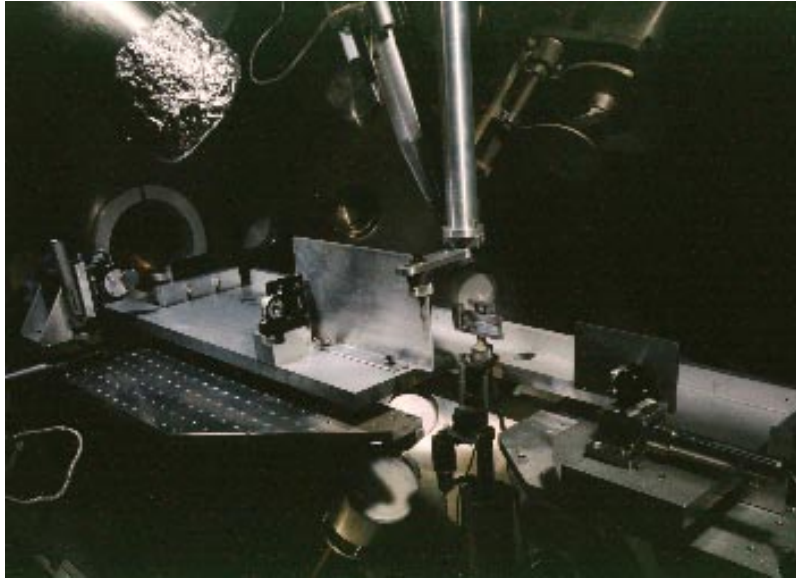
reconsideration of plans to close the LLNL Tritium Facility. Instead, the facility will be reconfigured to provide state-of-the-art tritium and radioactive decontamination research and development, with a tritium inventory capacity up to 5 grams. The PTPS is again playing a key supporting role in this new facility direction, this time providing tritium gas handling and glovebox cleanup capability. The system has proven so successful in this application that construction of a duplicate one is now planned.

Key Words: glovebox technology; Tritium Inventory Removal Project; tritium processing.



For further information please contact Mark Mintz (510) 422-8394 or Thomas Reitz (510) 422-9123.

X-Ray Lasers and High-Density Plasma



X-ray lasers are ideal for studying high-density plasmas of the sort produced by the Nova laser. We have demonstrated single-micrometer resolution of plasma images and interferometric techniques for determining plasma density. Current work on developing shorter pulses of x-ray laser light will improve resolution in two dimensions.

OVER the course of only a few decades, lasers have become ubiquitous. In the future, x-ray lasers are likely to become widespread because of their growing range of uses. Among other promising developments, x-ray lasers are being applied in areas ranging from biological imaging to materials science. One of our most recent and sophisticated uses of the x-ray laser is as a probe for imaging and understanding high-density plasmas.

Optical probes have been historically important in studying and characterizing laser-produced plasmas. However, researchers have had to overcome many obstacles in their attempts to analyze large, high-

density plasmas of the sort that can be created at LLNL by the Nova laser. The difficulties arise from several problems, including high absorption of the optical probe light, the adverse effects of refraction, and the impossibility of probing beyond critical densities in plasma. (Critical density, which is determined solely by the wavelength of the probe, is the electron density beyond which light of a given wavelength will not penetrate.)

Advances in high-energy, more reliable x-ray lasers together with improvements in mirror technology have made it possible to develop diagnostic techniques that are now suitable for evaluating the plasmas

of interest. This article reviews the status of laboratory x-ray lasers and their clear advantages in plasma diagnostics. It describes our three principal techniques: high-resolution imaging of the fine structure in plasma, moiré deflectometry used to measure density gradients in plasma, and interferometry for directly measuring electron density. Our recent work in the area of interferometry is made possible as a result of new beam splitter technology developed at LLNL. Finally, we discuss future applications for this important tool, including the characterization of plasmas that will be created by the proposed National Ignition Facility (NIF).¹

Photograph shows setup for generating an x-ray laser using one beam of the Nova laser.

About Plasmas

Researchers need detailed knowledge of the distribution of electron density in a laser-produced plasma for a wide range of endeavors. This type of information is essential for research in inertial confinement fusion, for laser-plasma interaction physics, and for interpreting high-temperature, high-density laboratory astrophysics experiments.

In laser-induced fusion, for example, a tiny capsule containing deuterium-tritium fuel (two heavy forms of hydrogen) is struck from all directions by radiant energy called the “drive.” In one arrangement known as direct drive, many powerful laser beams are focused so they impinge on the capsule. The rapid, rocketlike expansion of the capsule shell drives the inner portions of the capsule inward, compressing and heating the fuel. At a density of more than 200 g/cm^3 (more than a thousand times the density of solid hydrogen) and a temperature of about 100 million K (kelvin) (comparable to temperatures deep in the sun), a fuel plasma forms, and nuclear fusion reactions occur. In the next several decades, fusion energy could become a clean and limitless alternative to our current reliance on fossil fuels.

On Earth, plasma is a short-lived, highly or completely ionized gas that can be produced using several different types of targets. When high-intensity laser light irradiates a solid target, such as a metal foil, the extent of the plasma is determined by the laser spot size; therefore, plasmas can range from hundreds of micrometers to several millimeters in diameter. The plasma is also relatively long in the direction parallel to the drive laser, so an irradiated foil can span orders of

magnitude in density and temperature at a given time.

With each new laser system, we need increasingly sophisticated diagnostic instruments to “see” what is happening: as a function of the laser beam parameters (such as intensity and size), in targets of various types, and in the plasma. The central challenge in diagnosing such experiments is the ability to accommodate the spatial and time scales involved. The phenomena we are interested in occupy spatial scales from a single micrometer (about one-hundredth the diameter of a human hair) to a few millimeters, and time scales from several picoseconds (the time it takes light to move about a millimeter) to several nanoseconds. The plasma density can range from about 10^{20} to 10^{26} cm^{-3} ,* where solid density is about 10^{23} cm^{-3} . The electron densities we are interested in approach 10^{22} cm^{-3} .

We can obtain electron density information in many different ways. Examples include x-ray spectroscopy, absorption and scattering of incident laser light, and ultraviolet interferometry. However, each of these techniques has limitations, including the range of densities and scale sizes that can be measured. To overcome some of the limitations, we have developed several techniques based on a soft x-ray laser beam. Whereas the details of our techniques differ, they all have one central feature in common: they involve creating one plasma with one beam of Nova as a source of coherent x rays to image or diagnose a second plasma produced when a target is irradiated by another Nova beam.

What Is an X-Ray Laser?

The human eye sees only a small portion of the electromagnetic

spectrum, namely, wavelengths extending from about 700 nm for red light to about 400 nm for violet light (a nanometer is one billionth of a meter). At shorter wavelengths beyond violet light is the ultraviolet region that is invisible to the unaided eye and associated with potentially skin-damaging rays of the sun. X rays are a form of penetrating electromagnetic radiation with even shorter wavelengths ranging from about 10^{-6} to 10^2 nm. The soft x rays various researchers are using as a probe lie just beyond the ultraviolet portion of the spectrum and have wavelengths of a few to tens of nanometers.

X rays can be generated by accelerating electrons to high velocities and then stopping them suddenly by collision with a solid body. This technique produces short-wavelength x rays that can be dominated by radiation from atomic inner-shell transitions. Electron bombardment is the technique used for generating medical x rays.

In recent years, researchers have developed many different schemes for producing a laser of x rays. The most successful of the schemes has been collisionally pumped x-ray lasers, which are produced in plasmas containing ions in a highly charged state. Within the ions, electrons move between the ground state and various higher energy levels so that the conditions are achieved for producing x rays. The [box on p. 11](#) explains in more detail the principles behind lasers and collisional pumping schemes for generating a soft-x-ray laser.

In practical terms, collisionally pumped x-ray lasers are highly useful because they can operate over a wide range of pump conditions and with a variety of targets. Moreover, the

*This is the conventional mathematical expression of electron density in a given volume. In this instance, it records how many electrons are contained in 1 cubic centimeter.

range of wavelengths over which collisionally pumped soft-x-ray lasers operate (about 3.5 to 40 nm) make them good candidates for many different applications.

For our work in plasma diagnosis, we selected the neonlike yttrium x-ray laser. The name itself says a good deal about how the device functions. The atomic number of yttrium is 39, so it normally contains 39 protons and an

equal number of electrons. In a neonlike yttrium laser, yttrium is stripped of 29 of its 39 electrons, leaving 10 electrons, like neon.

In our laser, the x rays are produced by using high-intensity optical laser light to irradiate a cold lasant material, as shown in [Figure 1](#). Whereas the lasant material in various types of lasers can be a solid, liquid, or gas, the material we irradiate is

either a 3-cm-long plastic foil coated with a thin layer of yttrium or a solid slab of yttrium. We irradiate the yttrium with one of the ten beams of the Nova laser. When the intense optical laser light interacts with the lasant material, a very hot (approximately 10^7 K) cylindrical plasma is produced. X-ray laser amplification takes place along this plasma column.

What We Mean by a Collisionally Pumped X-Ray Laser

To produce a laser, the lasing material (lasant) must be put in the proper state; then the individual atoms (or ions) of the lasant must be properly prepared and then stimulated into emitting a photon at the laser wavelength. In each lasing atom, preparation is accomplished by adding energy to the atom so that an electron (usually the outermost electron in the atom) is excited to the upper lasing level, which is generally a metastable, or relatively long-lived, state. This is called pumping.



The excited atom can be induced to make a transition to the lower lasing level if the atom interacts with a photon possessing an energy equal to the energy difference between the two lasing levels. In the process of making the transition, the de-exciting atom emits a photon with this same energy. The emitted photons end up being in phase with each other; i.e., they are coherent. The emitted photon can induce the emission of additional photons (of energy and phase) in other already-pumped atoms. Additionally, each can be pumped again if the atom can be returned to its initial state, so the lower lasing level is usually very short-lived. This exponential increase in the number of photons in a given direction (called gain) gives rise to a large amount of coherent directed energy; this is a laser. In general, the more lasant atoms and the longer the laser, the brighter the resulting laser beam.

Most commercially available lasers use gases or lasing atoms suspended in a solid (such as glass) or a liquid. The pumping mechanism for these lasers is a bright light source (such as a flashlamp) that emits photons of the right wavelength to excite the lasing atoms to the upper lasing level. This is called photopumping. It is not a viable method of making an x-ray laser, however, because a very bright (and unavailable) source of x rays would be required to pump the atoms. Moreover, excitation produced in neutral atoms by x rays involve inner shell electrons (electrons interior of the outermost electron). In this situation, it is difficult to find a state to serve as an upper lasing level because the atom is very unstable.

The trick is to ionize the atoms first, removing many of the outer electrons so that excitation of the ions occurs in the remaining outer shell. These transitions can be at x-ray wavelengths. In our collisionally pumped x-ray laser, the ionization is accomplished by heating the lasant very quickly to high temperatures using one beam of the Nova laser focused to form a line, creating a long (a few centimeters), thin (a hundredth of a centimeter) plasma. This heating puts the lasant in the proper state to be pumped (for yttrium, 29 of the 39 electrons are removed). Pumping the ions is not performed by an outside x-ray source; it is done by the unbound electrons. The energetic electrons collide with the ions, thus creating a collisionally pumped x-ray laser. Lasing can then occur along the line of plasma. Finding the combination of material, ionization state, temperature, electron density, and lasing levels that will produce an x-ray is challenging.

Notice in **Figure 1** that the three-dimensional plasma we create is relatively long (3 cm) but not very wide (approximately 120 μm) or high

(approximately 500 μm). It is only in the long direction—along the line of the plasma—that x-ray photons interact with enough other excited

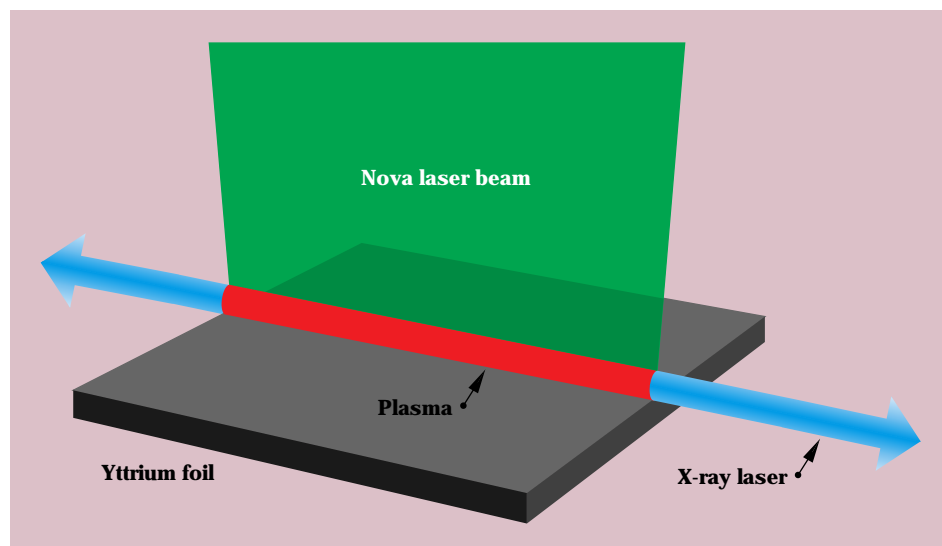
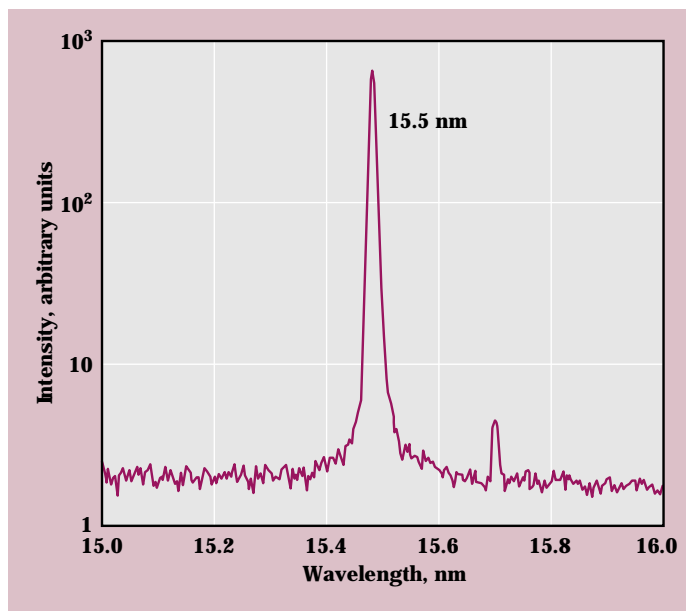


Figure 1. X rays are produced when a beam of high-intensity laser light from Nova bombards a plastic foil coated with a thin layer of yttrium. In our setup, the lasing medium we create is a very hot (approximately 10^7 K), uniform, and cylindrical plasma that is relatively long (3 cm) but only about 120 μm wide and 500 μm high. The lasing photons interact with enough other excited atoms only in the long direction (that is, along the 3-cm plasma line) to produce more photons, resulting in amplification. X-ray laser light emerges from both ends of this plasma line, but not in other directions.

Figure 2. This curve shows that the output of our yttrium x-ray laser is dominated by a single line, or monochromatic spike, at a wavelength of 15.5 nm. Such monochromatic light from a neonlike yttrium laser makes it well suited for studies of laser-produced plasmas.



atoms to produce more photons, resulting in amplification. The result is that our x-ray laser emerges from both ends of the plasma line, but not in other directions. The x-ray laser is coherent because a stimulated photon is similar to (has the same phase as) the photon that stimulates it.

X-ray lasers have several features that make them ideal for studying dense plasmas. First, the short wavelength of such lasers provides decreased refraction and greater penetration, compared to other longer-wavelength optical probes. As shown in **Figure 2**, the operating wavelength of our neonlike yttrium laser is dominated by a single line, or monochromatic spike, at 15.5 nm. We have produced multilayer mirrors for use in our experiments that are highly reflective at this wavelength.

A second advantage has to do with brightness. In imaging systems, brightness is one of the most important factors, and yttrium x-ray lasers are unequalled in this regard.² The high brightness of x-ray lasers makes them particularly well suited for imaging bright sources, such as a laser-produced plasmas.

A third advantage arises from the fact that our x-ray probe is, indeed, a laser. This means that we can exploit the coherence properties of the x-ray laser, in particular, as a density diagnostic.

A potential limitation of collisionally pumped x-ray laser systems has to do with their output pulse lengths. When the pulse is relatively long, a few hundred picoseconds, considerable motion can take place in the plasmas we want to investigate. Such motion can cause blurring in an image. We have been developing ways to generate the short pulses (with durations of less than 50 ps) needed for extending diagnostic techniques. Our recent work on decreasing the pulse duration is described toward the end of this article.

Direct Imaging of Plasmas

Two fundamental issues in high-resolution imaging are the wavelength of the probe and refraction in the medium being imaged. In general, shorter-wavelength probes allow us to see an object better, with ideal optical systems achieving resolutions comparable to the wavelength of the probe. At present with our imaging system, we are imaging structures as small as $1\ \mu\text{m}$, but we can do better in the future.

As shown in **Figure 3**, refraction is a change in the direction of light that occurs when light passes through a density gradient, that is, through material in which the index of refraction changes. Refraction can be a substantial problem in imaging because the amount of refraction, or bending of light, increases directly with the magnitude of the density gradient and the length along the gradient. Conversely, the amount of refraction decreases with increasing critical density, which is solely determined by the wavelength of the light. The rule to remember is that shorter-wavelength light generally penetrates much farther into a plasma and is less affected by gradients.

Currently, we are using the neonlike yttrium x-ray laser to image high-density, large plasmas of interest to the laser-fusion and astrophysics communities. In the past, probing high-density or large plasmas was difficult. With the yttrium laser, a broader range of electron densities and plasma lengths is accessible to us, as shown in **Figure 4**. By using short-wavelength (15.5-nm) light, we can reduce the adverse effects of refraction and probe plasma densities up to $10^{23}\ \text{cm}^{-3}$. Beyond this density, imaging is limited primarily by absorption.

Figure 5 shows our setup for high-resolution imaging experiments. To

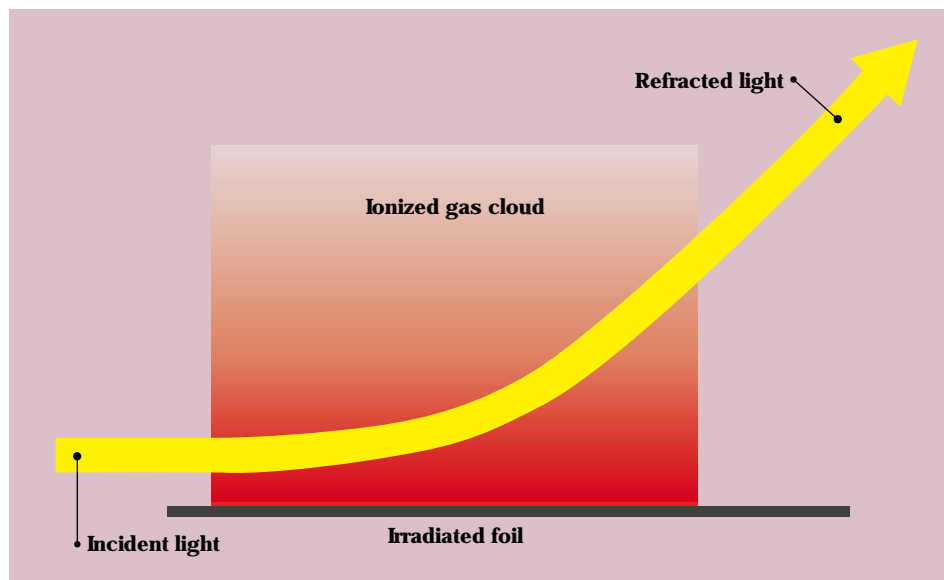


Figure 3. When light passes through material in which the index of refraction changes, the light changes direction. As shown here, the amount of refraction, or bending of light, increases directly with the magnitude of the density gradient and the length along the gradient. In our work, the density gradient is a “cloud” of highly ionized gas, that is, a plasma produced when we irradiate a target. In general, shorter-wavelength light penetrates much farther into such a plasma and is less refracted by gradients.

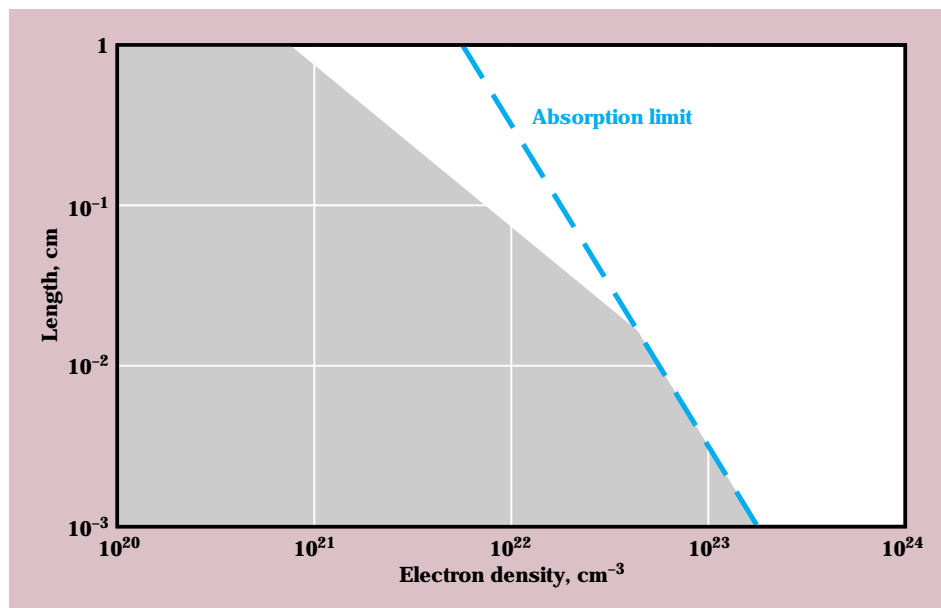


Figure 4. The shaded area shows the broad range of electron densities and plasma lengths that are accessible to us by using the yttrium x-ray laser. With its short-wavelength (15.5-nm) light, we can probe plasma densities up to $10^{23}\ \text{cm}^{-3}$. Beyond this density, imaging is primarily limited by absorption. (At lower densities, the number of fringe shifts that can be resolved via interferometric techniques becomes the constraint.)

use an x-ray laser fully as a plasma diagnostic, we must include optical elements, such as mirrors. Notice that the setup in **Figure 5** uses a sequence of two multilayer mirrors. The x-ray beam is first collected with a spherical multilayer mirror that collimates the beam so that it does not converge or

diverge appreciably. This collimated beam backlights the laser-produced plasma formed when a target, such as a foil, is irradiated by another optical laser beam from Nova (the second beam is shown at the top of **Figure 5**). An image of the plasma is focused by a second spherical multilayer mirror

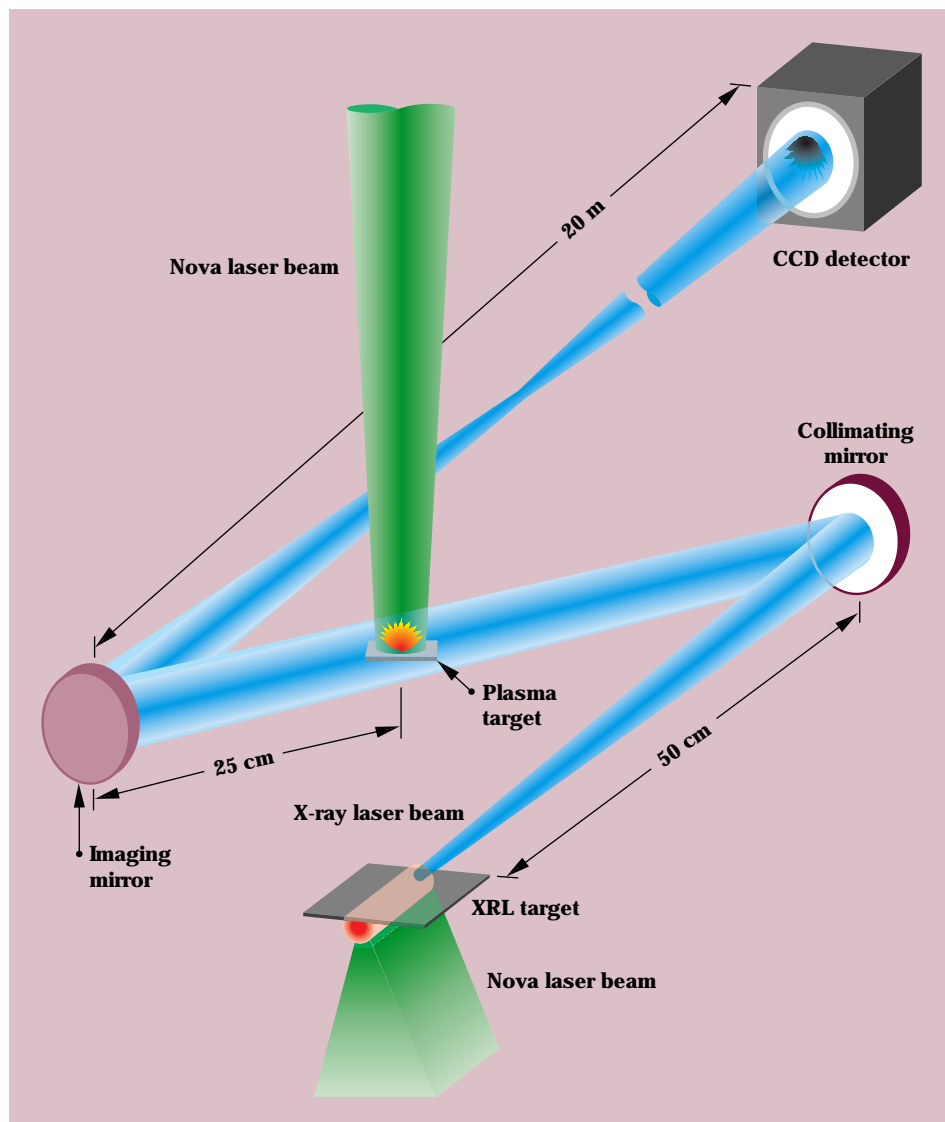


Figure 5. Experimental setup for directly imaging plasma. We use two beams of Nova, one to create the x-ray laser and another to produce a plasma. The yttrium x-ray laser beam (formed at the bottom) backlights the target. This beam is first collected and collimated by the multilayer mirror on the right. As the sample target is irradiated by another beam of the Nova laser (center), the backlit plasma image is formed by a second multilayer mirror (left) and is focused onto the backside of a highly sensitive charge-coupled device (CCD) detector (top right).

onto a charge-coupled device (CCD) detector that has high sensitivity to x rays and high dynamic range.

One potentially serious problem in our type of imaging system is that multilayer mirrors can be damaged by side-scattered laser light, especially when distances are short (less than 25 cm from mirror to plasma) and the laser light is intense. We have solved the problem by locating highly reflective mirrors 50 cm away from the plasma and by using only a small part of each mirror, shielding the remainder of the mirror. Multilayer mirrors are essentially crystals with layer spacings that are matched to the wavelengths being diagnosed. Our multilayer mirrors consist of 15 layer pairs of molybdenum and silicon, and they have a measured reflectivity at 15.5 nm of about 60% at normal incidence. High reflectivity is essential because the mirrors must be efficient in a complex optical system.

At our highest magnification (30 \times) the spatial resolution of our imaging system is better than 1 μm . The resolution is limited by the CCD detector and by spherical aberrations caused by the mirrors.

Figure 6 shows an image of a 10- μm -thick polyethylene (CH) foil overcoated with 3 μm of aluminum and irradiated with a 1-ns pulse of intense green light (10^{14} W/cm 2) from the Nova laser. The foil was illuminated on the polyethylene side, where the CH serves as an ablator, similar to the function of a fusion capsule. We backlit this foil with a 150-ps pulse from the yttrium x-ray laser. **Figure 6** is what we call a side-on image of the foil and plasma where the top of the picture corresponds with the foil's exploding rear surface. In this view, the Nova laser pulse comes from the bottom of the picture, and the x-ray pulse comes from behind the plane of the object to serve as a backlighter.

This image of an “accelerated” foil shows density perturbations on the foil’s rear surface. At first, we hypothesized that the fine 5- to 6- μm structures visible in the side-on image might be small plasma filaments, which are sometimes seen in other kinds of experiments. Our imaging system, with its approximately 1- μm spatial resolution (along the x axis in Figure 6) was clearly able to resolve the structures, but an important question remained: exactly what would account for such perturbations? Repeated shots gave similar results. It seemed possible that the structure could arise from nonuniformities of the target mass or from techniques used to smooth the Nova laser beam.

More recently, we have concluded that the foil itself is breaking up as a result of the Nova beam imprinting its near-field beam intensity pattern on the foil. This finding could have important implications for inertial fusion target development for direct-drive experiments. Shots performed with smoother Nova beams show reduced filamentation. We will soon begin to take face-on images of exploding foils (where the foil’s front surface is essentially driven toward the detector) to get another perspective on what is happening.

Notice that in Figure 6, the spatial resolution along the flight path of the foil (that is, along the vertical axis) is limited by the duration of the x-ray laser pulse. For a pulse about 200 ps in duration, which is typical in our work, we obtain a longitudinal resolution ranging from a few to 20 μm . Obviously, it would be desirable to improve the resolution along the flight path. This desire is just one of the reasons why developing a shorter-pulse x-ray laser is important.

We have also used our imaging system to study x-ray-heated foils. In this work, we use one Nova beam to illuminate a thin gold foil from which

high-energy x rays heat an aluminum target foil placed 1 mm away. The smooth expansion of the aluminum we have observed agrees well with earlier computer simulations.

One drawback of direct plasma imaging is that we need an accurate estimate of opacity to determine the electron densities of plasmas. At the wavelengths of soft-x-ray lasers and with the metal targets we are using, such estimates can be difficult to make. Thus, we have developed two alternative techniques. Moiré deflectometry allows us to measure electron density gradients, and

interferometry allows us to measure electron density itself directly.

Moiré Deflectometry

Moiré deflectometry is a relatively recent technique that has been widely used to measure many different physical phenomena. Deflectometry can be applied to characterize optical components, to study the dynamics of fluid flow, and to measure variations in plasma density.

Deflectometry measures the refraction of a collimated beam of light passing through a medium or

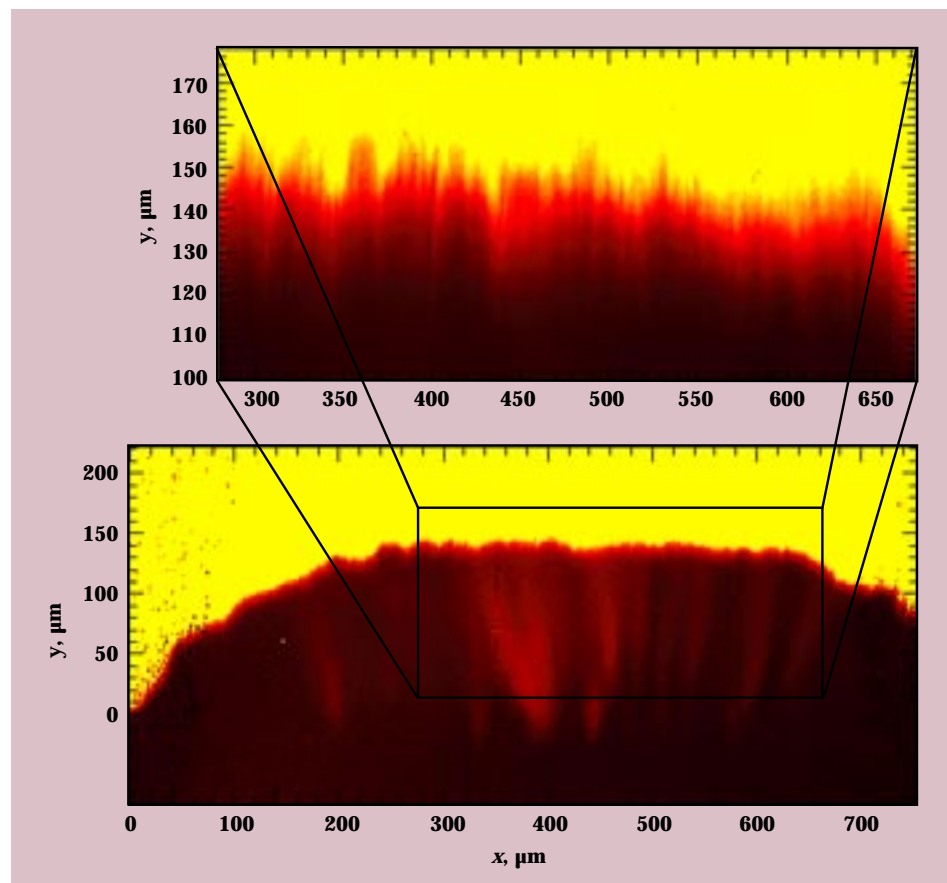


Figure 6. X-ray laser image of an exploding 10- μm foil overcoated with 3 μm of aluminum and irradiated with a 10^{14}-W/cm^2 beam of the Nova laser. The picture is a side-on view of the central region of the foil plasma, which is being driven upward. The foil was originally located at zero on the vertical scale. The resolution of the image is about 1 μm along the x axis. The plasma structure shows both large- and small-scale electron density perturbations, which may arise from breakup of the foil.

subject of interest. In our case, the collimated probe beam is a set of intense x rays that are nearly parallel. As in our direct-imaging work, we use the yttrium x-ray laser beam to probe millimeter-scale, laser-produced plasmas.³ Previous work using visible

and ultraviolet probe beams has been limited by excessive refraction. Our soft-x-ray laser provides the desired short-wavelength probe beam to avoid the problem.

When a probe beam passes through a pair of evenly spaced stripes

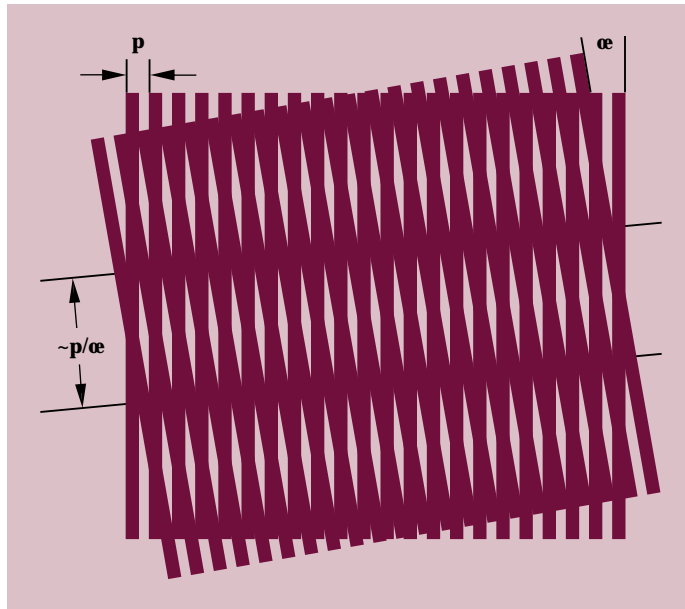
(gratings) that are offset and rotated slightly with respect to one another, a moiré pattern is created. The moiré pattern, as shown in Figure 7, is a set of dark regions, or fringes, corresponding to the stripe intersections and lighter regions that are the open areas in between the stripes. In everyday experience, we see moiré patterns if we look through a double-screen door or window. Normally, we don't see all the details of such patterns; instead, we observe a smooth set of fringes or lines. Such is the case in our work.

If we look through a pair of gratings at an angle, the fringes are shifted from the original position they had in a perpendicular view. In moiré deflectometry, we can exploit the fringe shifts, and the connection between the angle of refraction and electron density, to obtain a measure of the electron density gradient along a plasma. To do so, we simply placed a pair of offset gratings just before the CCD detector in the experimental setup (Figure 5). We also added a combination of flat mirrors and a filter to the setup so that the detector would see a narrow range of radiation centered at 15.5 nm. We control the sensitivity of the deflectometer by varying the distance separating the gratings.

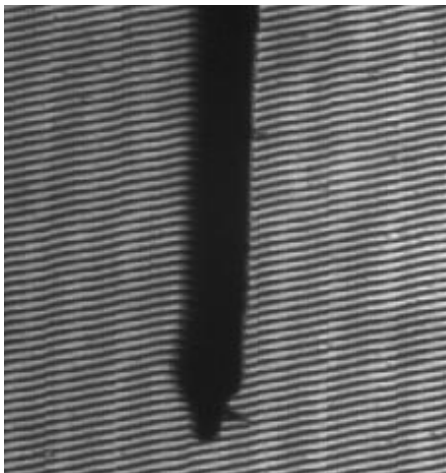
First, we created a deflectogram by using the x-ray beam, a CH target, and a pair of gratings without any plasma present. In this control experiment, the second beam of Nova was not used, so no target plasma was created to deflect the fringes. Figure 8a shows the control image, which consists of a uniform moiré pattern except where the beam was blocked by the side of the CH target.

Next, we obtained a deflectogram of a CH plasma. As in the control experiment, we used a 5-mm-square, 50- μm -thick CH foil, but this time, we irradiated the foil with the Nova

Figure 7. A moiré pattern, consisting of a set of dark bands or fringes, is produced when two one-dimensional gratings are overlaid and rotated slightly with respect to one another. By locating a pair of offset gratings like these just before the CCD detector in our experimental setup, we can measure the deflection of the fringes to obtain an electron density gradient along a plasma.



(a)



(b)

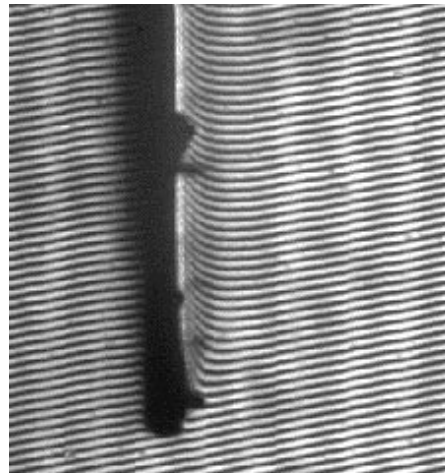


Figure 8. Two deflectograms of a polyethylene (CH) target viewed from the side. (a) A control image with no plasma present shows the expected unperturbed moiré pattern. (b) A deflectogram of a laser-irradiated CH foil target illuminated from the right side. This image shows distinct fringe shifts close to the target surface. We can use the deflections to infer the electron density gradient near the surface. The dark features associated with the target surface are probably caused by ripples in the CH material.

laser. The pulse duration of the x-ray laser was about 200 ps, which is short enough to avoid significant blurring. In this experiment, the x-ray beam passed through the plasma about 1 ns after the start of irradiation. To maximize fringe shifts and demonstrate our ability to probe relatively large plasmas, we used a large, 3-mm-diameter Nova laser spot on the CH target.

Figure 8b is a deflectogram of a CH plasma. In areas that are far from the surface of the foil, which is once again viewed from the side, this image shows the expected unperturbed moiré pattern. Closer to the surface, fringe shifts (or displacements) by as much as about four fringe spacings are visible. Immediately adjacent to the surface, the fringes disappear because contrast is lost to very strong density gradients. (We can reduce this limitation by increasing the magnification and reducing the separation between rulings.) Subsequent analysis of the deflectogram—which assumes we know the boundary density far from the target surface—allows us to infer a density of slightly greater than $4 \times 10^{21} \text{ cm}^{-3}$ near the foil surface.

It is noteworthy that this type of deflectometry can be done with probes that are much weaker than our intense yttrium x-ray laser. In fact, the intensity could be reduced by a factor of 25, and the image quality would still be acceptable. By making other modifications, such as reducing the thickness of filters used in our setup, we could optimize the system even further. This ability means that it should be possible to produce a deflectogram with low-energy x-ray laser systems, such as those that use selenium or germanium.

The primary disadvantage of deflectometry is that it gives us a measurement of the plasma density gradient, not the plasma density. The desired density measurement can be made by interferometry.

Interferometry

Our most recent technique is, in some respects, also our most useful tool in terms of its potential applications. Because an observed fringe shift is directly proportional to the electron density in a plasma being probed by interferometry, this tool can provide a direct measurement of density in two dimensions.

The technique of interferometry adds a reference beam to the system. The interference of the reference beam and the probe beam supplies information directly on the index of refraction of the target. Such an approach requires the use of beam splitters that are effective at x-ray laser wavelengths. Recently, LLNL researchers have developed and fabricated such beam splitters with reflectivity in the range of about 25% and transmission of about 20%. The beam splitters are similar to our multilayer mirrors and consist of eight layer pairs of molybdenum and silicon on a 100-nm-thick silicon nitride support. Our current beam splitters have a 1-cm-square aperture, and we are working on 2-cm-square apertures.

Figure 9 shows the experimental setup for soft-x-ray interferometry. In the terminology of optics, the arrangement includes a Mach-Zehnder interferometer. In essence, we add four multilayer mirrors to the setup we used for direct plasma imaging. Two of the mirrors are semitransparent (the beam splitters) and two are completely reflecting. Whereas the probe beam passes through the plasma, the reference beam does not. When the two beams recombine after the probe passes through the plasma, they interfere. The interference shows up as fringes on the detector. By measuring the number of fringe shifts and using the known values of the x-ray wavelength and the plasma path

length, we can calculate the electron density from a simple equation.

In a control experiment, we obtained an interferogram without using the second beam of Nova to produce a target plasma. The results showed excellent fringe contrast and proved the viability of the technique.

Figure 10 is an interferogram we obtained after irradiating a 10-mm-thick coating of CH on a polished silicon substrate. The CH coating, viewed from the side in this image, was irradiated from the top of the picture with the Nova laser. For this experiment, the laser spot size was about $700 \mu\text{m}$ in diameter, and the intensity of the beam was $2.7 \times 10^{13} \text{ W/cm}^2$. By counting the fringe shifts that are clearly visible above the CH surface in the center of the spot, we find that the maximum electron density is $3 \times 10^{21} \text{ cm}^{-3}$. This value and the overall density profile of the plasma are in good agreement with computer simulations.

Current Work and Future Applications

Ultimately, the spatial resolution of a plasma image in two dimensions is limited by the duration of the x-ray laser pulse. Therefore, to obtain better images and improved measurements of plasma density, we need to improve the x-ray laser itself.

In work that is in progress to reduce the pulse duration, we have begun to irradiate thin yttrium foils with multiple optical laser pulses. The first Nova pulse, which has less energy than those that follow, heats the thin foil target to produce a plasma. The subsequent pulses ionize the preformed plasma to produce conditions suitable for generating shorter-duration x-ray pulses.

When using multiple pulses in this way, we need to overcome the anticipated problem of limited gain

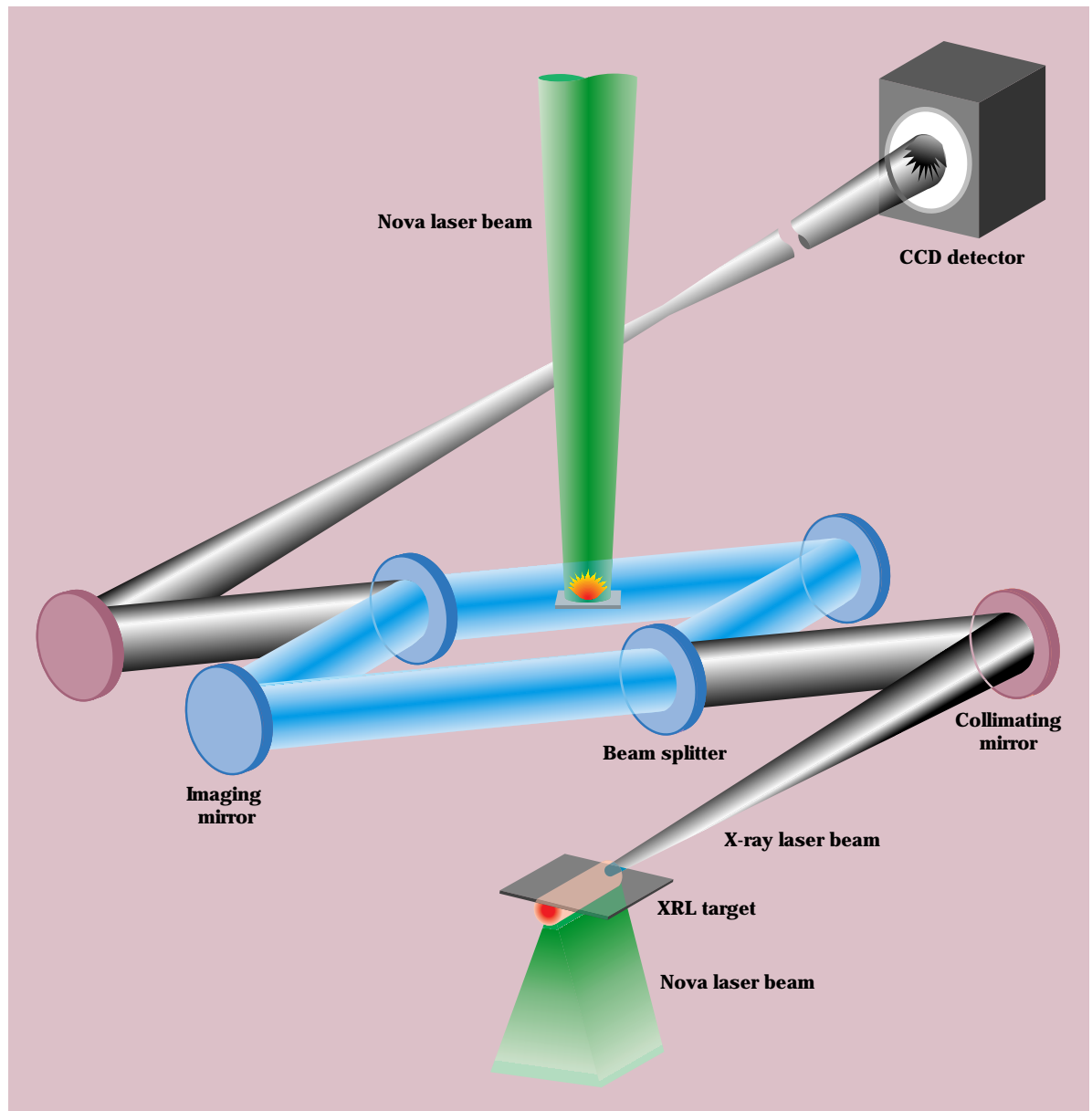
(or brightness). One way to shorten the x-ray laser pulse and to maintain brightness at the same time is to use a so-called traveling wave. In this approach, the incident Nova wave front is tilted by inserting a grating so that the pulse, in effect, is swept along the 3-cm foil target. The technique matches the optical pump (the Nova pulse) to the propagation of the x-ray

pulse along the plasma. Our early efforts have yielded an x-ray laser pulse duration of 45 ps.⁴ To our knowledge, this is the shortest collisionally pumped x-ray laser to date. In the future, we expect to achieve pulse durations of less than 20 ps.

In the future, our x-ray laser can be applied as a probe to study the very

dense plasmas that will be created at the proposed National Ignition Facility (NIF). The NIF would allow us to extend collisionally pumped neonlike and nickel-like x-ray laser systems to shorter wavelengths and high output energies, which would make the x-ray laser an even more important diagnostic tool. For example, we estimate that we will be able to

Figure 9. Experimental setup for soft-x-ray interferometry. This arrangement is essentially identical to that used for plasma imaging, but it also includes a Mach-Zehnder interferometer (shown in blue), which adds two multilayer mirrors and two multilayer beam splitters. We align the interferometer using white light.



achieve wavelengths of about 2 nm and peak intensities of 1×10^{17} W/cm².

The short-pulse capabilities of NIF will also allow us to investigate a variety of new x-ray laser schemes, including recombination x-ray lasers. In recombination lasers, an atom is first stripped of several electrons, and then some of those electrons recombine with the ion into the upper lasing level. Recombination systems have long been viewed as an alternative to collisionally pumped systems, offering the potential for higher conversion efficiencies. To date, however, such systems have proven inefficient, in part because it is difficult to produce long, uniform plasmas suitable for x-ray propagation. A facility the size of NIF would allow recombination x-ray systems to be tested adequately.

Finally, x-ray lasers are well suited for a variety of other applications ranging from biological imaging to nonlinear optics. In the area of biological imaging, for example, x-ray microscopy offers a way to study wet, thick specimens with a demonstrated resolution that is about five times better than that of conventional optical microscopes. Electron microscopes are limited to thin samples (the limit is about 0.4 μm in thickness), and they cause radiation damage to and decomposition of the specimens being studied. In contrast, x-ray lasers have the potential to produce high-contrast, high-resolution images of whole cells or other structures that are 2 to 10 μm thick before significant damage occurs to the specimen.

Key Words: interferometry; moiré deflectometry; National Ignition Facility (NIF); plasma imaging; x-ray laser—plasma diagnostics.

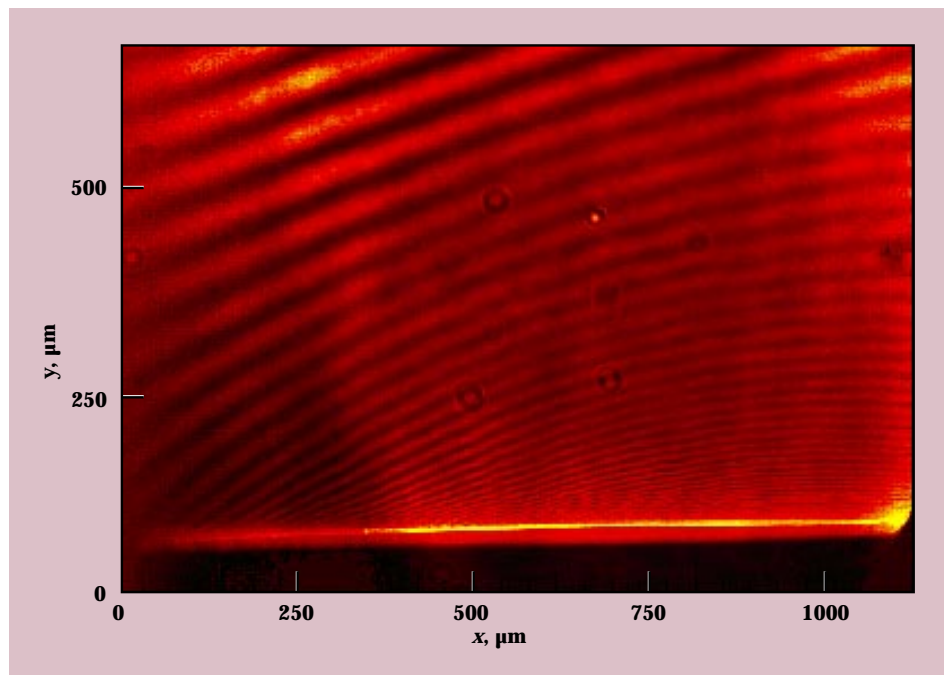
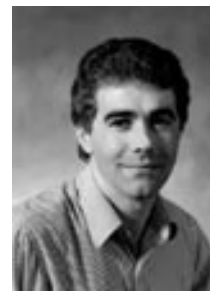


Figure 10. Interferogram of a laser-heated CH foil shown in a horizontal orientation and viewed from the side. The Nova drive laser, which produced the target plasma, is incident from the top of the picture. The fringe shifts are clearly visible just above the foil surface. One fringe shift corresponds to an electron density of 2×10^{20} cm⁻³. By counting the shifts, we have determined that the maximum electron density near the foil surface is 3×10^{21} cm⁻³.

Notes and References

1. For further reading on the proposed National Ignition Facility, see the December 1994 issue of *Energy and Technology Review*, UCRL-52000-94-12.
2. L. B. Da Silva, B. J. MacGowan, S. Mrowka, J. A. Koch, R. A. London, D. L. Matthews, and J. H. Underwood, "Power Measurements of a Saturated Yttrium X-Ray Laser," *Optics Letters* **18**, 1174 (1993).
3. D. Ress, L. B. Da Silva, R. A. London, J. E. Trebes, S. Mrowka, R. J. Procassini, T. W. Barbee, Jr., and D. E. Lehr, "Measurement of Laser-Plasma Electron Density with a Soft X-Ray Laser Deflectometer," *Science* **265**, 514 (1994).
4. L. B. Da Silva, R. A. London, B. J. MacGowan, S. Mrowka, D. L. Matthews, and R. S. Craxton, "Generation of a 45 ps Duration 15.5 nm X-Ray Laser," *Optics Letters* **19**, 1532 (1994).



For further information contact Luiz B. Da Silva (510) 423-9867, Robert C. Cauble (510) 422-4724, or Stephen B. Libby (510) 422-9785.

Silicon Carbide Microcomponents

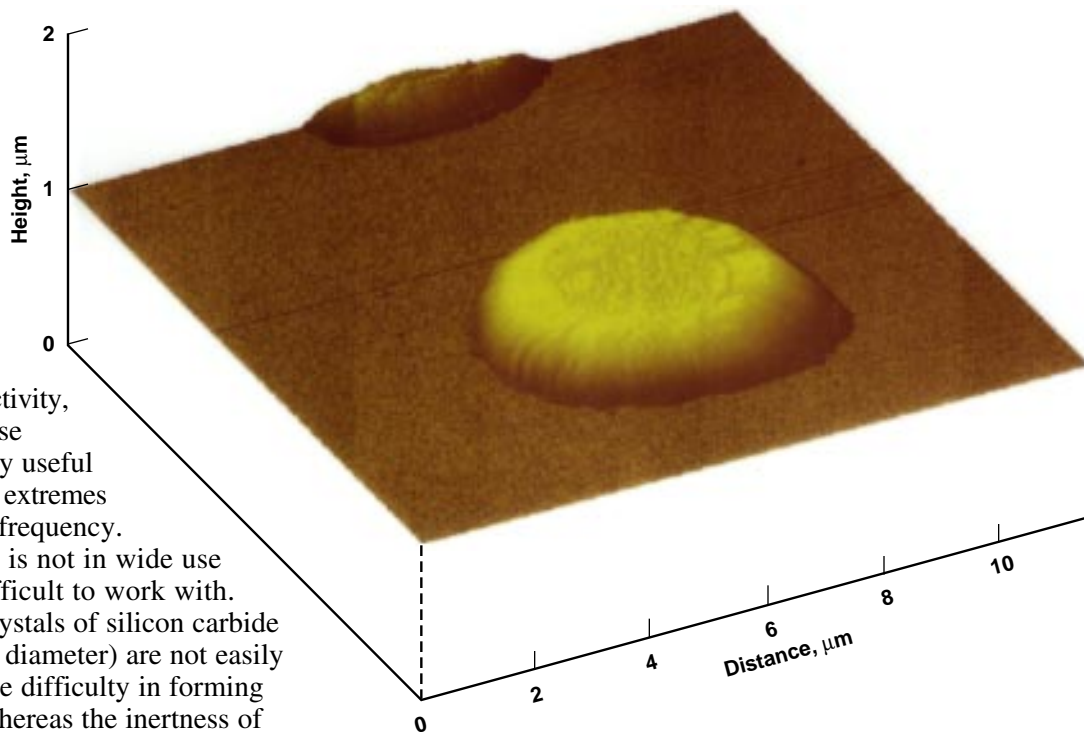
SILICON carbide is a highly promising material for many semiconductor applications. Among other advantages, this material has excellent physical stability and hardness, great strength at high temperature, high thermal conductivity, and a low friction coefficient. These characteristics make it particularly useful for integrated circuits operating at extremes of temperature, power, speed, or frequency.

Unfortunately, silicon carbide is not in wide use today because it is extremely difficult to work with. One problem is that large-area crystals of silicon carbide (approximately 10 centimeters in diameter) are not easily grown. Another has to do with the difficulty in forming the necessary microstructures. Whereas the inertness of silicon carbide is an important attribute, this property also makes it difficult to etch silicon carbide so that microstructures can be formed. Dry etching techniques are both slow and problematic, as are chemical-vapor deposition techniques.

In breakthrough research that opens up new civil, defense, and space applications for semiconductors, we have developed a technique for manufacturing silicon carbide microchips. Such chips can withstand high temperatures and demanding operating conditions, making them ideal for use in automobile and aircraft engines, among other applications. The elegance of the new approach is that it combines existing silicon technology with the unique way that the fullerene, C_{60} , can react with a heated silicon surface.

The carbon molecules, known as buckminsterfullerenes, and commonly called “buckyballs” because their shape resembles the geodesic dome created by Buckminster Fuller, are the third member of the pure

Atomic-force micrograph of a silicon carbide dot on a silicon test wafer. The dot is 5 μm in diameter and about 1 μm high. Microstructures such as this can be repositioned on a silicon wafer by using the tip of an atomic-force microscope.



carbon family, which includes diamond and graphite as the two more commonly known family members. The molecule C_{60} has a perfect soccer-ball-like structure that can open like the petals of a tulip under certain circumstances.

The technique developed at LLNL takes advantage of the fact that C_{60} molecules react with a silicon surface heated between 950 and 1250 K (kelvin) to form silicon carbide. The C_{60} molecules, however, do not react with a silicon dioxide surface heated to the same temperature.

In our new approach, standard lithographic techniques are first applied to deposit a controlled pattern of silicon dioxide to a thickness of about 1 micrometer (μm) on a silicon wafer. After the wafer is heated to 1100 K, it is exposed to a beam, or flux, of C_{60} vapor for about an hour. The carbon molecules stick to the bare silicon and essentially bounce off the oxide. To remove the unwanted silicon dioxide, the wafer is then dipped in concentrated hydrofluoric acid. The end result is a silicon wafer with a silicon carbide microstructure in place.

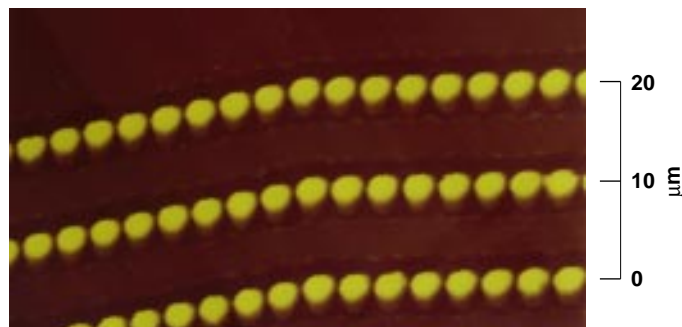
In the past year, we have grown films of silicon carbide to thicknesses greater than 1 μm . To measure the height of silicon carbide areas, we use atomic force microscopy and apply a tip-to-surface force in the range of 10^{-9} N (newtons). The illustration on the previous page shows an atomic-force micrograph of a 5- μm -diameter dot of silicon carbide on one of our test structures.¹ Because the adhesion of silicon carbide films thicker than 1 μm on a silicon wafer is relatively weak, we can also use the tip of an atomic force microscope to apply a slightly greater force (in the range of 10^{-8} N) so that we can maneuver a microcomponent to a desired location on the wafer. We have maneuvered components ranging from 50 to about 1.5 μm in diameter in this way. We have also produced patterns of silicon carbide, as shown in the illustration at right.

In a related effort, we used our new procedure to coat the tip of a silicon atomic-force microscope with a thin (approximately 0.5- μm) layer of silicon carbide.² We have found that C_{60} has large surface mobility and is able to diffuse into areas that are not in the direct line of sight of the beam of applied vapor. Thus, the tip of the atomic-force microscope was uniformly coated even though some of the surfaces were inclined at various angles with respect to the C_{60} source. We found that the sharpness of the tip remained basically unchanged after it was coated.

Silicon carbide microcomponents have strong potential in a variety of applications because of their unique physical properties. Although silicon carbide will not replace silicon chips, and the material may not be suitable for some electrical uses, it has the practical benefit of surviving extreme mechanical and thermal conditions. For example, it could be applied to detect flameouts in aircraft engines by measuring pressure and temperature in the engine quickly enough to stop and then restart the engine.

In recent research, we have also determined that silicon carbide microcomponents may also have a use in solving friction and wear problems encountered at crucial junctures in microelectromechanical systems (MEMS).³ These very tiny sensors, actuators, resonators, and even motors rely on standard silicon processing technology. Their operation can be limited by the relatively rapid wear of contacting silicon surfaces and other mechanical properties.

To assess the usefulness to MEMS of silicon carbide microcomponents made by the process described above,



We have achieved selective patterned growth of crystalline silicon carbide. These rows of 2- μm -diameter silicon carbide dots are about 10 μm apart.

we tested the mechanical properties relevant to the longer life of MEMS—coefficient of friction, hardness, and elastic modulus—with modified atomic-force microscopes and a Nanoindenter. The results suggest that when used in MEMS, these films of silicon carbide grown from C_{60} may lessen wear and improve operation. The coefficient of friction for the silicon carbide film was one-half to one-third that of the silicon currently in use, and its hardness, based on a compared elastic modulus of the two materials, was almost 12 times greater. Silicon carbide films grown from C_{60} may, therefore, present yet another opportunity for application previously not considered.

References

1. A. V. Hamza, M. Balooch, and M. Moalem, "Growth of Silicon Carbide Films via C_{60} Precursors," *Surface Science* **317**, L1129 (1994).
2. M. Balooch and A. V. Hamza, "SiC Microcomponents via Reaction of C_{60} with Silicon," *Journal of Vacuum Science and Technology B* **12**(6), 1 (1994).
3. Kathryn Morse, T. P. Weihs, A. V. Hamza, M. Balooch, Z. Jiang, and D. B. Bogy, *Nanomechanical Properties of SiC Films Grown from C_{60} Precursors Using Atomic Force Microscopy*, Lawrence Livermore National Laboratory, Livermore, CA, UCRL-JC-119657 (1995). This article has been submitted for publication to the *Journal of Tribology—Transactions of the American Society of Mechanical Engineers*.

For further information contact Alex V. Hamza (510) 422-3073 or Mehdi Balooch (510) 422-7311.

Modern Technology for Advanced Military Training

ON June 8, 1994, two U.S. helicopters left the deck of an aircraft carrier and flew inland close to earth over enemy territory. Their route took them through a mountain pass and just above enemy forces moving both on and off road. The mission objective was to rescue a six-member special operations team that had been previously deployed under cover of darkness to take out a SCUD missile site. During pickup, various skirmishes occurred, but the special operations team was rescued and transported safely to a friendly airfield.

Perhaps the most remarkable feature of the operation was that the helicopters never left the U.S.—or the ground. Although each helicopter was “flown” by a live pilot, the hardware, in reality, consisted of high-fidelity virtual simulators, and the rescue was a military training exercise. The demonstration linked LLNL’s Joint Conflict Model (JCM) with other recent technological advances to create a computer-simulated rehearsal of a military operation.

The exercise addressed a recommendation that had been made by the Defense Science Board two years earlier. The Board sought to demonstrate that modern technologies capable of creating a synthetic battlefield environment could provide enhanced training for Armed Services personnel. Proposals were solicited from the Unified Commanders-in-Chief, the Armed Services, and Department of Defense agencies for simulations that would match the recommended technologies against operational needs.

In response, LLNL researchers worked with Martin Marietta Corporation under the sponsorship of the Joint

An off-road tank as viewed by a pilot from his simulator cockpit (left). Topographic map of the terrain, with enemy forces in red and friendly forces in blue, as viewed by the Joint Conflict Model operator (right).



WarFighting Center, under whose direction JCM was originally developed. This team put together a proof-of-principle project that linked virtual aircraft simulators at Kirtland Air Force Base in Albuquerque, New Mexico, with LLNL’s theater-level war game, JCM, installed at Hurlburt Field in Fort Walton Beach, Florida.

The official name of the demonstration was the SOFNET–JCM Interface Project. (SOFNET stands for Special Operations Forces Simulation Network.) The main goal of the project was to create and share a seamless, synthetic battlefield environment that integrated virtual simulations (the helicopters) and a constructive simulation (our JCM) across a wide-area distributed network. Each of five specific objectives represented an important advance in creating synthetic battlefields:

- To achieve cost-effective, live interplay between the two different kinds of simulations.
 - To allow entities controlled by JCM to be visible to crews in the helicopter simulators.
 - To allow real-time, context-correct interactions among sensors and targeting, weapons fire, and damage effects.
 - To permit modeling control to be transferred between simulations.
 - To resolve important differences between the models so that terrain and other effects looked realistic.
- All the objectives were met.

Kirtland's SOFNET of aircraft simulators provided the high-resolution, realistic military hardware. In its normal configuration, the Kirtland system consists of three helicopter simulator cockpits and a training observation center. Each simulator features a full-motion base and six degrees of freedom. The observation center, with its 41-seat multimedia auditorium, can display on large screens the out-the-window image of a helicopter simulator.

The second principal component of the demonstration, our JCM, is a theater-level war game. It features software tools to create a battle scenario, follow the battle's progress, and keep crews informed about the effects of their own actions and the responses of an enemy. In technical terms, JCM is referred to as an entity-based constructive simulation because it involves a software representation of opposing forces using rules to depict real-life situations. The designation "constructive" also implies a rich simulation that can model many devices or entities as opposed to the few components usually associated with a virtual simulation.

Our extensive experience in developing and testing JCM since 1991 has proven that its design is both robust and easily enhanced—that is, it can readily accommodate the addition of new features. JCM can function either interactively as a training simulation system or in batch mode as an analytic tool. When it operates in the interactive mode with human players, the speed is

synchronized to a real-time clock. Up to 24 computer workstations can participate in a simulation, and each workstation supports one or two players. The players can use interactive, color-based planning menus to create operational battle plans and then transmit them to any other workstation in the exercise.

When JCM operates in the batch mode, on the other hand, it runs at top speed to complete replications rapidly. In this mode, it is limited only by the capability of the host computer. A complete history of each exercise is maintained. Quick analysis of current and past exercises can provide insights within minutes—a task that could take months not so long ago.

For the 45-minute demonstration that took place in June 1994, LLNL was responsible for designing a Distributed Interactive Simulation (DIS) interface for JCM. DIS is a powerful and evolving protocol that conforms to IEEE (Institute of Electrical and Electronics Engineers) standards. In essence, the interface we developed allows our war game to talk to and understand the other elements participating in the exercise, notably the virtual simulators at Kirtland and real players. Similarly, a DIS interface to SOFNET was developed by Kirtland's contractor, Martin Marietta Corporation, for simulator work. To tie the network together, we used an interconnecting, encrypted T-1 link operating at 1.5 megabits per second. The link was divided into



View of the training observation center at Kirtland Air Force Base. Participants in an exercise can see out-the-window views from the perspective of one or more helicopter pilots. The screen just to the right of center displays our Joint Conflict Model while it is being run by an operator.

channels to provide both video teleconferencing and transmission of simulation data. We also installed a second JCM suite for backup at Kirtland. Once the connections were made, the participants in New Mexico and Florida could see what was happening at both locations, an added benefit for this advanced demonstration.

Although we solved many complex problems, the issue of terrain correlation merits mention. Both JCM and SOFNET use a database to create pictures that approximate the real world. However, SOFNET uses a mesh of three-dimensional polygons to represent terrain, whereas our model uses an array of elevation grid posts. Because the formats are different, it was necessary to correlate altitudes between the two databases. If, for example, the soldiers and aircraft we can simulate with JCM were not properly correlated with SOFNET terrain, then an entity on the ground could have been seen from a helicopter cockpit as being either below or above ground. After several attempts were made to address this problem, we eventually solved it by requiring the network interface to first accept our ground-based data and then to pass on altitude corrections to SOFNET.

In an era of shrinking budgets, the demand for fast, flexible, high-fidelity simulation systems that can link training crews in different locations will grow steadily. The SOFNET–JCM Interface Project serves as a testbed and springboard for future work. It confirms our ability to bring unique experience to tasks such as aircrew training, mission planning, and command-and-control coordination. It also enables special-forces aircrews to rehearse missions as abstract war games or in preparation for real-world situations. Furthermore, JCM has applications in areas other than war, such as disaster relief and drug interdiction. This project shows that emerging technologies can enhance training and reduce system development costs.

 *For further information contact
Mike Uzelac (510) 422-4812 or
JoAnn Matone (510) 424-6048.*

The LLNL Portable Tritium Processing System

The end of the Cold War significantly reduced the need for facilities to handle radioactive materials for the U.S. nuclear weapons program. The LLNL Tritium Facility was among those slated for decommissioning. The plans for the facility have since been reversed, and it remains open. Nevertheless, in the early 1990s, the cleanup (the Tritium Inventory Removal Project) was undertaken. However, removing the inventory of tritium within the facility and cleaning up any pockets of high-level residual contamination required that we design a system adequate to the task and meeting today's stringent standards of worker and environmental protection. In collaboration with Sandia National Laboratory and EG&G Mound Applied Technologies, we fabricated a three-module Portable Tritium Processing System (PTPS) that meets current glovebox standards, is operated from a portable console, and is movable from laboratory to laboratory for performing the basic tritium processing operations: pumping and gas transfer, gas analysis, and gas-phase tritium scrubbing.

The Tritium Inventory Removal Project is now in its final year, and the portable system continues to be the workhorse. To meet a strong demand for tritium services, the LLNL Tritium Facility will be reconfigured to provide state-of-the-art tritium and radioactive decontamination research and development. The PTPS will play a key role in this new facility.

Contacts: Mark Mintz (510) 422-8394 or Thomas Reitz (510) 422-9123.

X-Ray Lasers and High-Density Plasma

The improved reliability, high brightness, and short wavelength of x-ray lasers make them ideally suited for studying large, high-density plasmas of interest to the laser-fusion research community. We have been developing the neonlike yttrium x-ray laser as a probe, together with the necessary multilayer mirrors and beam splitters, to image plasmas produced at the Nova laser facility and to measure electron density. With its short-wavelength (15.5-nm) light, we can use the yttrium x-ray laser to probe plasma densities up to 10^{23} cm^{-3} . At the highest magnification (30 \times), the spatial resolution of our imaging system is better than 1 μm . Using the technique of moiré deflectometry, we have measured density gradients in plasmas. Using the technique of interferometry, we have probed 3-mm-long plasmas with electron densities up to $3 \times 10^{21} \text{ cm}^{-3}$. Temporal blurring of plasma images remains the main limitation of our approach. Thus, we are continuing to improve our theoretical and experimental understanding of laboratory x-ray lasers. We are currently working on techniques to reduce the blurring of images by shortening the x-ray laser pulse to durations approaching about 20 ps. In the future, this important research tool can be applied to study high-density plasmas produced at the proposed National Ignition Facility. Other important applications of the x-ray laser include biological imaging of whole, live cells and other structures at resolutions superior to those obtainable by conventional optical microscopy.

Contacts: Luiz B. Da Silva (510) 423-9867, Robert C. Cauble (510) 422-4724, or Stephen B. Libby (510) 422-9785.

